Inorg. Chem. **2005**, *44*, 6409–6414

Inorganic Chemistry Article

Structure Determination and Relative Properties of Novel Cubic Borates $MM'_4(BO_3)_3$ (M = Li, M′ = Sr; M = Na, M′ = Sr, Ba)

L. Wu, X. L. Chen,* H. Li, M. He, Y. P. Xu, and X. Z. Li

Beijing National Laboratory for Condensed Matter Physics, Institute of Physics, Chinese Academy of Sciences, Beijing 100080, China

Received February 27, 2005

A series of novel borates, $MM'_4(BO_3)_3$ (M = Li, M′ = Sr; M = Na, M′ = Sr, Ba), have been successfully synthesized by standard solid-state reaction. The crystal structures have been determined from powder X-ray diffraction data. They crystallize in the cubic space group $Ia\bar{3}d$ with large lattice parameters: $a = 14.95066(5)$ Å for $LiSr_4(BO_3)_3$, $a = 15.14629(6)$ Å for $NaSr_4(BO_3)_3$, and $a = 15.80719(8)$ Å for $NaBa_4(BO_3)_3$. The structure was built up from 64 small cubic grids, in which the M′ atoms took up the corner angle and the BO_3 triangles or MO_6 cubic octahedra filled in the interspaces. The isolated $[BO_3]^{3-}$ anionic groups are perpendicular to each other, distributed along three ⟨100⟩ directions. The anisotropic polarizations were counteracting, forming an isotropic crystal. Sr and Ba atoms were found to be completely soluble in the solid solution $NaSr_{4-x}Ba_x(BO_3)_3$ ($0 \leq x \leq 4$). The photoluminescence of samples doped with the ions Eu^{2+} and Eu^{3+} was studied, and effective yellow and red emission was detected, respectively. The results are consistent with the crystallographic study. The DTA and TGA curves of them show that they are chemically stable and congruent melting compounds.

Introduction

Inorganic borates have long been a focus of research for their variety of structure type, wide spectrum with high damage threshold, and high optical quality. Studies of alkali-metal and alkaline-earth-metal borates have produced a large family of compounds with outstanding physical properties.[1−6] Recently, photoluminescence are found in many rare earth ion doped alkaline-earth-metal borates.[7−11] Some have been used as useful phosphors, such as UV-emitting Eu^{2+}:SrB_4O_7 in lamps for medical applications and skin tanning.[7] Because of the similar radii and same valence with Sr^{2+} and Ba^{2+}, Eu^{2+} is easy to replace some sites of Sr and Ba atoms in crystal cell, and then photoluminescence can be found in the doped compounds. These properties depend on the crystal structures of these borates with a variety of BO atomic groups. The various structures and properties inspirit us to explore more borates in the systems $M_2O-M'O-B_2O_3$ (M = Li, Na; M′ = Sr, Ba) to search for new functional materials. Six new compounds, $LiSr_4(BO_3)_3$, $NaSr_4(BO_3)_3$, $NaSrBO_3$, $Na_3SrB_5O_{10}$, $NaSrB_5O_9$, and $NaBa_4(BO_3)_3$ were synthesized successfully. The powder XRD patterns of them have been submitted for publication in the Powder Diffraction File (International Centre for Diffraction Data) in 2003 or 2004. Three of the six new borates, $LiSr_4(BO_3)_3$, $NaSr_4(BO_3)_3$, and $NaBa_4(BO_3)_3$, are isostructural and have been structure determined from powder X-ray diffraction data. What makes the structures remarkable is that they all crystallize in the cubic system, which is very rare in borate (about 1.18% of PDF compounds contain boron and oxygen and even less in borate[12]). The structural character of borates is different from that of alloys, in which all the atoms prefer to be close-packed, and then easy to crystallize in the cubic

* Author to whom correspondence should be addressed. E-mail: xlchen@aphy.iphy.ac.cn. Tel.: +86 10 82649039. Fax: +86 10 82649646.

(1) Berker, P. *Adv. Mater.* **1998**, *10*, 979−992.
(2) Chen, C. T.; Ye, N.; Lin, J.; Jiang, J.; Zeng, W. R.; Wu, B. C. *Adv. Mater.* **1999**, *11*, 1071−1078.
(3) Chen, C. T.; Wu, B. C.; Jiang, A.; You, G. *Sci. China B* **1985**, *18*, 235−243.
(4) Chen, C. T.; Wu, Y.; Jiang, A.; Wu, B. C.; You, G.; Li, R.; Lin, S. *J. Opt. Soc. Am. B* **1989**, *6*, 616−621.
(5) Chen, C. T.; Wang, Y.; Wu, B.; Wu, K.; Zeng, W.; Yu, L. *Nature* **1995**, *373*, 322−324.
(6) Hu, Z.; Higashiyama, T.; Yoshimura, M.; Mori, Y.; Sasaki, T. *Z. Kristallogr.* **1999**, *214*, 433−434.
(7) Pei, Z. W.; Su, Q. *J. Alloys Compd.* **1993**, *198*, 51−53.
(8) Schaffers, K. I.; Keszler, D. A. *Inorg. Chem.* **1994**, *33*, 1201−1204.
(9) Diaz, A.; Keszler, D. A. *Mater. Res. Bull.* **1996**, *31*, 147−151.
(10) Diaz, A.; Keszler, D. A. *Chem. Mater.* **1997**, *9*, 2071−2077.
(11) Penin, N.; Seguin, L.; Touboul, M.; Nowogrocki, G. Synthesis and crystal structure of three $MM'B_9O_{15}$ borates (M = Ba, Sr and M′ = Li; M = Ba and M′ = Na). *Int. J. Inorg. Mater.* **2001**, *3*, 1015−1023.
(12) *Findit*, version 1.3.3; Fachinformationzentrum: Karlsruhe, Germany, 2002−2004.

10.1021/ic050299s CCC: $30.25
Published on Web 07/23/2005

Table 1. Crystallographic Data, Experimental Details of X-ray Powder Diffraction, and Rietveld Refinement Data for $LiSr_4(BO_3)_3$, $NaSr_4(BO_3)_3$, and $NaBa_4(BO_3)_3$

param	$LiSr_4(BO_3)_3$	$NaSr_4(BO_3)_3$	$NaBa_4(BO_3)_3$
fw	533.85	549.85	748.68
cryst system	cubic	cubic	cubic
space group	$Ia\bar{3}d$	$Ia\bar{3}d$	$Ia\bar{3}d$
$a = b = c$ (Å)	14.95066(5)	15.14629(6)	15.80719(8)
V (Å^3)	3341.80(3)	3474.71(4)	3949.69(6)
Z	16	16	16
d_c (g cm^{-3})	4.243	4.203	5.034
diffractometer	MXP21VAHF/M21X, MAC Science	MXP21VAHF/M21X, MAC Science	MXP21VAHF/M21X, MAC Science
radiatn type	Cu Ka	Cu Ka	Cu Ka
wavelength (Å)	1.5418	1.5418	1.5418
profile range (deg in 2θ)	10−130	10−120	10−120
step size (deg in 2θ)	0.02	0.02	0.02
no. of observns (N)	6000	5500	5500
no. of contributg reflcns	502 ($K\alpha_1 + K\alpha_2$)	452 ($K\alpha_1 + K\alpha_2$)	509 ($K\alpha_1 + K\alpha_2$)
no. of struct params (P_1)	12	12	12
no. of profile params (P_2)	16	16	16
R_{Bragg} (%)	7.00	7.16	7.43
R_p (%)^a	6.09	8.62	10.6
R_{wp} (%)^a	8.11	12.4	14.4
R_{exp} (%)^a	3.14	3.47	8.57
S^a	2.6	3.6	1.7

^{a} Note: $R_p = \sum|y_{io} - y_{ic}|/\sum|y_{io}|$, $R_{wp} = [\sum w_i(y_{io} - y_{ic})^2/\sum w_i y_{io}^2]^{1/2}$, $R_{exp} = [(N - P_1 - P_2)/\sum w_i y_{io}^2]^{1/2}$, and $S = \sum[w_i(y_{io} - y_{ic})^2/(N - P_1 - P_2)]^{1/2}$.

crystal system. But in borate, especially when the fundamental building unit is anisotropic polarized planar BO_3 groups, isotropic crystals can be expected only if the BO_3 groups are distributed in a particular manner. Just as that for the three new compounds, isolated $[BO_3]^{3-}$ anionic groups are perpendicular to each other, distributed along the ⟨100⟩ directions, and anisotropic polarizations were counteracted. Beyond the three isostructural novel compounds, a solid solution region $NaSr_{4-x}Ba_x(BO_3)_3$ ($0 \le x \le 4$) was confirmed as existing.

In addition, because of the similar radius of Eu ion and Sr/Ba ions, photoluminescence was expected in the Eu^{2+} and Eu^{3+} doped new compounds. The broad-band luminescence $4f^6 5d^1 \rightarrow 4f^7$ of Eu^{2+} is strongly host dependent with emission wavelengths extending from the UV to the red portions of the spectrum. As to the Eu^{3+} ion, although it has a valence different from that of Sr^{2+} and Ba^{2+} ions, a small quantity of doping is expected to be successful. In this study, the photoluminescence of Eu^{2+}-doped $LiSr_4(BO_3)_3$ and Eu^{3+}-doped $MM'_4(BO_3)_3$ (M = Li, M′ = Sr; M = Na, M′ = Sr, Ba) was investigated.

Experimental Section

Solid-State Syntheses. Polycrystalline samples $MM'_4(BO_3)_3$ (M = Li, M′ = Sr; M = Na, M′ = Sr, Ba) were prepared by using sintering at high-temperature solid-state reaction. Stoichiometric mixtures of high-purity Li_2CO_3, $SrCO_3$, and H_3BO_3 (LiSr), Na_2CO_3, $SrCO_3$, and H_3BO_3 (NaSr), and Na_2CO_3, $BaCO_3$, and H_3BO_3 (NaBa) were heated at 750, 800, and 830 °C, respectively, with several grinding steps of the samples between heatings. The powder samples were characterized by powder XRD. Pure $LiSr_4(BO_3)_3$, $NaSr_4(BO_3)_3$, and $NaBa_4(BO_3)_3$ were obtained, and the two sodium borates were found to be isostructural with $LiSr_4(BO_3)_3$. Samples for the solid solution $NaSr_{4-x}Ba_x(BO_3)_3$ ($0 \le x \le 4$) were prepared with the same reagents and a heating period of 90 h at 830 °C. The isostructural $LiBa_4(BO_3)_3$ was also confirmed to exist but with some unconquerably impure peaks.

To exploit the possibility of using the $LiSr_4(BO_3)_3$, $NaSr_4(BO_3)_3$, and $NaBa_4(BO_3)_3$ as a host of luminescent materials, a series of Eu-doped samples $LiSr_4(BO_3)_3$:$x$$Eu^{2+}$, $LiSr_4(BO_3)_3$:$x$$Eu^{3+}$, $NaSr_4(BO_3)_3$:$x$$Eu^{3+}$, and $NaBa_4(BO_3)_3$:$x$$Eu^{3+}$ were prepared. $LiSr_4(BO_3)_3$:$x$$Eu^{2+}$ were prepared from suitable stoichiometric ratio of high-purity Li_2CO_3 (AR), $SrCO_3$ (AR), Eu_2O_3 (99.99%), and H_3BO_3 (>99.99%). The well-mixed mixture was baked at 600 °C in a H_2 (8%) + Ar (92%) reducing atmosphere for 8 h. The baked sample was thoroughly ground and baked again at 900 °C in the same atmosphere for 48 h. Eu^{3+}-doped $LiSr_4(BO_3)_3$, $NaSr_4(BO_3)_3$, and $NaBa_4(BO_3)_3$ samples were prepared with the same reagents by heating mixtures in air.

Structure Determination. The data for $LiSr_4(BO_3)_3$ used for structure determination were collected over a 2θ range of 10−130° in the step scan mode with a step size of 0.02° and a measurement time of 1 s/step at room temperature, and the data for $NaSr_4(BO_3)_3$ and $NaBa_4(BO_3)_3$ used for Rietveld refinement were collected from 10 to 120° in the same mode. Additional technical details are given in Table 1. The diffraction patterns of the three compounds were indexed using DICVOL91.[13] This gave out an cubic unit cell with a = 14.941(2) Å for $LiSr_4(BO_3)_3$, a = 15.138(5) Å for $NaSr_4(BO_3)_3$, and a = 15.796(2) Å for $NaBa_4(BO_3)_3$. The systematic absences of hkl with $h + k + l = 2n + 1$, $0kl$ with $k = 2n + 1$ and $l = 2n + 1$, hhl with $2h + l = 4n + m$, and $h00$ with $h = 4n + m$ (m = 1−3) suggest that the possible space group is $Ia\bar{3}d$. All the three compounds are isostructural.

The whole pattern of $LiSr_4(BO_3)_3$ was decomposed using the Fullprof program[14] on the Le Bail method,[15] and a total of 397 independent $|F_o|$ values were extracted. The finally agreement factors converged to R_B = 2.62%, R_p = 5.62%, R_{wp} = 8.29%, and R_{exp} = 3.17%. Lattice parameters were refined to be a = 14.95093(8) Å. Direct method were applied with the SHELXL97 program package[16] to the extracted $|F_o|$. According to the atom distances,

(13) Boultif, A.; Louer, D. *J. Appl. Crystallogr.* **1991**, *24*, 987−993.
(14) Rodriquez-Carvajal, J.; Fernadez-Diaz, M. T.; Martinez, J. L. *J. Phys.: Condens. Matter* **1991**, *3*, 3215−3234.
(15) Le Bail, A.; Duroy, H.; Fourquet, J. L. *Mater. Res. Bull.* **1988**, *23*, 447−452.
(16) Sheldrick, G. M. *SHELXS97 and SHELXL97*; University of Göttingen: Göttingen, Germany, 1997.

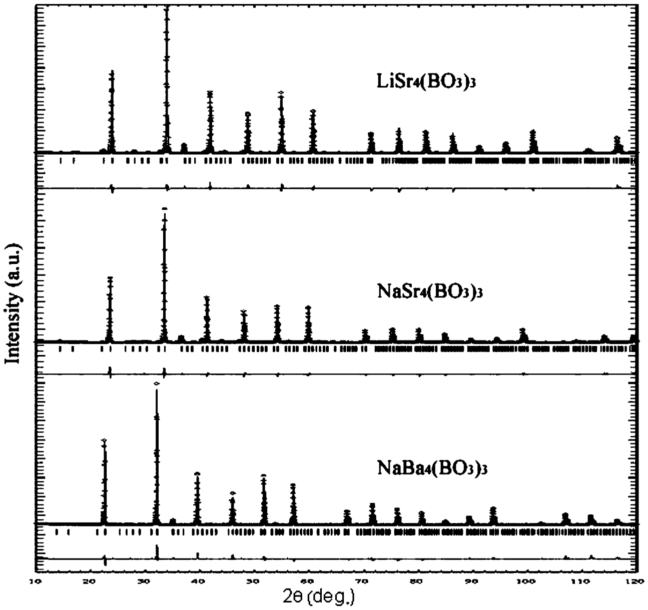

Figure 1. Final Rietveld refinement plots of the three compounds $LiSr_4(BO_3)_3$, $NaSr_4(BO_3)_3$, and $NaBa_4(BO_3)_3$. Small circles (○) correspond to experimental values, and the continuous lines, the calculated pattern; vertical bars (|) indicate the positions of Bragg peaks. The bottom trace depicts the difference between the experimental and the calculated intensity values.

three peaks listed in the *E*-map were likely to correspond to the correct positions of atoms; two were assigned to Sr atoms, and the other was assigned to the Li atom. The other atoms were located by using difference Fourier synthesis. In this course, once an atom was located, it would be used for the next run of difference Fourier synthesis. At last, a satisfactory rough structure was obtained, and then it was refined using the Rietveld method[17,18] within the Fullprof program. In the final cycles of refinement a total of 28 parameters were refined (12 structural parameters and 16 profile parameters) and the finally agreement factors converged to $R_B = 7.00\%$, $R_p = 6.09\%$, $R_{wp} = 8.11\%$, and $R_{exp} = 3.14\%$. Lattice parameters were refined to be $a = 14.95066(5)$ Å. The structures of $NaSr_4(BO_3)_3$ and $NaBa_4(BO_3)_3$ were determined by Rietveld method on the basis of the structural model of $LiSr_4(BO_3)_3$. In the final cycle of refinement a total of 28 parameters were refined (12 structural parameters and 16 profile parameters) and the finally agreement factors converged to $R_B = 7.16\%$, $R_p = 8.62\%$, $R_{wp} = 12.4\%$, and $R_{exp} = 3.47\%$ for $NaSr_4(BO_3)_3$ and $R_B = 7.43\%$, $R_p = 10.6\%$, $R_{wp} = 14.4\%$, and $R_{exp} = 8.57\%$ for $NaBa_4(BO_3)_3$. Lattice parameters were refined to be $a = 15.14629(6)$ Å for $NaSr_4(BO_3)_3$ and $a = 15.80719(8)$ Å for $NaBa_4(BO_3)_3$. The final refinement patterns are given in Figure 1. The crystallographic data, fractional atomic coordinates, and equivalent isotropic displacement parameters are reported in Tables 1 and 2; significant bond lengths and angles are listed in Table 3.

Element Content Determination. The Li, Na, Sr, Ba, and B content in the compounds was determined by using the inductivity coupled plasma−atomic emission spectrometry (ICP-AES) technique.

Optical Measurement. The photoluminescence (PL) spectra were taken on a PTI-C-700 fluorescence spectrometer with a Xe lamp ($\lambda = 400$ nm) as the excitation source.

IR Spectra Measurement. Infrared spectra were recorded with a Perkin-Elmer 983 infrared spectrophotometer in the 300−1500-cm^{-1} wavenumber range using KBr pellets.

(17) Rietveld, H. M. *Acta Crystallogr.* **1967**, *22*, 151−152.
(18) Rietveld, H. M. *J. Appl. Crystallogr.* **1979**, *12*, 483−485.

Table 2. Fractional Atomic Coordinates and Equivalent Isotropic Displacement Parameters (Å^2) for $LiSr_4(BO_3)_3$, $NaSr_4(BO_3)_3$, and $NaBa_4(BO_3)_3$

	site	*x*	*y*	*z*	U_{eq}
Sr(1)	16a	0	0	0	0.0188(10)
Sr(2)	48f	0	0.25	0.00242(8)	0.0106(3)
O(1)	96h	0.1335(5)	0.2714(3)	0.1286(6)	0.007(1)
O(2)	48g	0.1769(4)	0.4269(4)	0.125	0.024 (3)
B	48g	0.1086(7)	0.3586(7)	0.125	0.003(5)
Li	16b	0.125	0.125	0.125	0.033(13)
Sr(1)	16a	0	0	0	0.0318(9)
Sr(2)	48f	0	0.25	0.00209(9)	0.0221(3)
O(1)	96h	0.1357(5)	0.2751(3)	0.1324(5)	0.028(2)
O(2)	48g	0.1773(5)	0.4273(5)	0.125	0.029(3)
B	48g	0.1096(7)	0.3596(7)	0.125	0.012(6)
Na	16b	0.125	0.125	0.125	0.017(3)
Ba(1)	16a	0	0	0	0.0218(10)
Ba(2)	48f	0	0.25	−0.00224(15)	0.0104(3)
O(1)	96h	0.1297(13)	0.2728(7)	0.1278(14)	0.017(3)
O(2)	48g	0.1716(9)	0.4216(9)	0.125	0.029(7)
B	48g	0.109(2)	0.359(2)	0.125	0.035(13)
Na	16b	0.125	0.125	0.125	0.021(6)

Differential Thermal Analysis. The melting behavior of the title compounds was investigated by differential thermal analysis (DTA). A DTA measurement was carried out with a CP-G high-temperature differential thermal instrument. The precision of measurement was ±3 °C. The heating rate was 10 °C/min from room temperature to 1250 °C.

Results and Discussion

Description of Crystal Structures. The $MM'_4(BO_3)_3$ (M = Li, M′ = Sr; M = Na, M′ = Sr, Ba) compounds crystallize in the cubic space group $Ia\bar{3}d$. As expected, the volume evolution follows the values of the ionic radii of the various M and M′ ions ($Li^+ < Na^+$ and $Sr^{2+} < Ba^{2+}$): $V_{LiSr} < V_{NaSr} < V_{NaBa}$ (Table 2). They show a novel structure type, and no other member of this structural family is found previously in borates. As illustrated in Figures 2 and 3, the fundamental building units of $MM'_4(BO_3)_3$ (M = Li, M′ = Sr; M = Na, M′ = Sr, Ba) are isolated planar $[BO_3]^{3-}$ groups, which are perpendicular to each other and distributed along the three directions: ⟨100⟩. The B−O bond lengths vary from 1.344(12) to 1.451(13) Å with an average value of 1.387 Å, and the O−B−O angles are between 117.5(3) and 124.51(9)°. These values are normal in a BO_3 plane triangle. The M atoms are coordinated with six oxygen atoms, forming MO_6 cubic octahedra (M = Li or Na in the following text). The periodic characteristic of the structure can be seen with more clarity from Figure 3. The BO_3 triangles and MO_6 cubic octahedra are located at the centers of cubic grids consisting of eight M′ (M′ = Sr or Ba in the following text) atoms; moreover, every two MO_6 cubic octahedra are separated from three interperpendicular BO_3 triangles along any one of the three directions and share corners with the adjacent BO_3 triangles. The M′ atoms appear in two crystallographically different environments, as shown in Figure 4. The M′(1) atoms (in the 16a position) are coordinated to six oxygen atoms, forming distorted octahedral, while the M′(2) atoms (in the 48f position) are eight-coordinated to oxygen atoms, forming two-capped trigonal prisms and sharing planes and edges with the adjacent $M'(2)O_8$ polyhedra and $M'(1)O_6$ octahedra, respectively. In the three compounds, the obvious

Table 3. Selected Interatomic Distances (Å) and Angles (deg) for $LiSr_4(BO_3)_3$, $NaSr_4(BO_3)_3$, and $NaBa_4(BO_3)_3$

$LiSr_4(BO_3)_3$		$NaSr_4(BO_3)_3$		$NaBa_4(BO_3)_3$	
Sr(1)−O(1)6	2.535(7)	Sr(1)−O(1)6	2.512(6)	Ba(1)−O(1)6	2.733(17)
Sr(2)−O(2)2	2.442(5)	Sr(2)−O(2)2	2.465(6)	Ba(2)−O(2)2	2.624(12)
Sr(2)−O(1)2	2.619(6)	Sr(2)−O(1)2	2.682(6)	Ba(2)−O(1)2	2.793(16)
Sr(2)−O(1)2	2.693(7)	Sr(2)−O(1)2	2.725(6)	Ba(2)−O(1)2	2.864(17)
Sr(2)−O(1)2	2.765(8)	Sr(2)−O(1)2	2.875(7)	Ba(2)−O(1)2	2.927(22)
Li−O(1)6	2.193(7)	Na−O(1)6	2.283(5)	Na−O(1)6	2.35(1)
B−O(1)2	1.358(12)	B−O(1)2	1.344(12)	B−O(1)2	1.39(4)
B−O(2)	1.444(12)	B−O(2)	1.451(13)	B−O(2)	1.41(4)
O(1)−B−O(2)	119.04(9)	O(1)−B−O(2)	117.74(10)	O(1)−B−O(2)	121.3(2)
O(1)−B−O(2)	119.04(9)	O(1)−B−O(2)	117.74(10)	O(1)−B−O(2)	121.3(2)
O(1)−B−O(1)	121.92(9)	O(1)−B−O(1)	124.51(9)	O(1)−B−O(1)	117.5(3)

character of the cations is that the radii of alkali-metal cations are small and those of the alkaline-earth-metal cations are comparatively large, which make enough interspace for the cubic grids to place the MO_6 cubic octahedra. When potassium was introduced to replace the lithium and sodium or magnesium and calcium were introduced to replace the strontium and barium, no isostructural compound was found. We believe that the substitution of a larger alkali-metal cations for M or the substitution of a smaller alkaline-earth-metal cations for M′ will all make the structure unstable. Of course, too much difference between the size of M and M′ atoms will also make the structure unstable, which might be one of the reasons that the compound $LiBa_4(BO_3)_3$ is difficult to synthesize.

Infrared Spectra and Thermal Stability Analysis. To further confirm the coordination surroundings of B−O in the $MM'_4(BO_3)_3$ structure, the IR spectra of $LiSr_4(BO_3)_3$, $NaSr_4(BO_3)_3$, and $NaBa_4(BO_3)_3$ were measured at room temperature and given in Figure 5. The IR absorption at wavenumbers smaller than 500 cm^{-1} mainly originates from the lattice dynamic modes. The strong bands observed above 1100 cm^{-1} should be assigned to the B−O stretching mode of triangular $[BO_3]^{3-}$ groups, while the bands with maxima at about 700−800 cm^{-1} should be attributed to the B−O out of plane bending, which confirm the existence of the $[BO_3]^{3-}$ groups.[19] It is found that there are two peaks above 1100 cm^{-1}, which is believed to come from the two different bond lengths of B−O. Figure S1 represents the DTA and TGA curves of $LiSr_4(BO_3)_3$, $NaSr_4(BO_3)_3$, and $NaBa_4(BO_3)_3$. The peaks at about 945, 1175, and 1207 °C should be the melting points of $LiSr_4(BO_3)_3$, $NaSr_4(BO_3)_3$, and $NaBa_4(BO_3)_3$, respectively. The DTA and TGA curves of them show that they are chemically stable and probably congruent melting compounds, which suggest that crystals of them may be easily grown.

Solid Solution $NaSr_{4-x}Ba_xB_3O_9$ ($0 \le x \le 4$). Because of the similar radii of Sr and Ba, we investigated the binary phase region of $NaSr_4(BO_3)_3$ and $NaBa_4(BO_3)_3$. The powder X-ray diffraction patterns of the samples of solid solution $NaSr_{4-x}Ba_x(BO_3)_3$ ($0 \le x \le 4$) with the increased x are shown in Figure 6a. The linear relationship of the refined lattice parameters (Fullprof) with the solubility x was presented in Figure 6b. It is clear that Sr and Ba may completely substitute each other.

Photoluminescence. Figure 7a shows the luminescence spectra of $LiSr_4(BO_3)_3{:}xEu^{2+}$ in different Eu^{2+} concentrations. It shows a broad emission band with maximum near 590

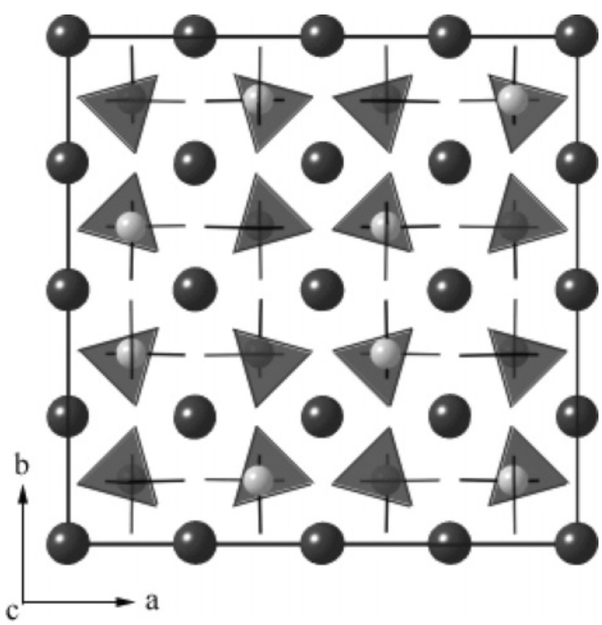

Figure 2. Structure projections of the $MM'_4(BO_3)_3$ compounds viewed along [001]. Big black balls represent M′ atoms. Black triangles are planar BO_3 triangles, and black short lines are their side faces. Grayish balls represent M atoms (M = Li, M′ = Sr; M = Na, M′ = Sr, Ba).

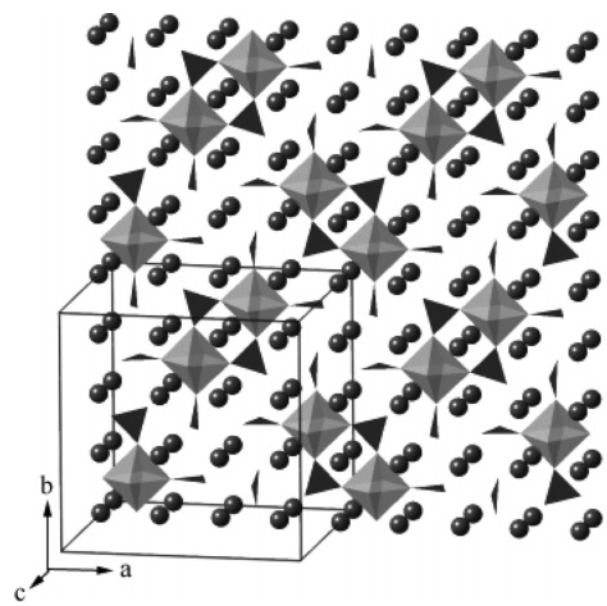

Figure 3. One layer of the crystal structure stacked from the MO_6 (M = Li or Na) octahedral and BO_3 triangles. More than one unit cell along the a and b axis ($-0.1 < a < 2.1$, $-0.1 < b < 2.1$) and less than one unit cell along the c axis ($-0.1 < c < 0.3$) are shown here for clarity.

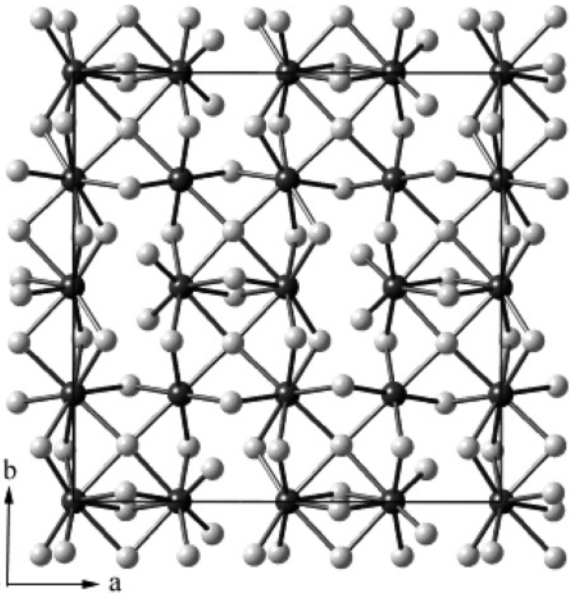

Figure 4. Coordination surroundings of M′ (M′ = Sr or Ba) with O atoms. Black balls represent M′ atoms, and grayish ones depict O atoms. B and M (M = Li or Na) atoms are omitted, and only one layer of the crystal structure ($-0.2 < a < 1.2$, $-0.2 < b < 1.2$, $0.1 < c < 0.4$) is shown here for clarity.

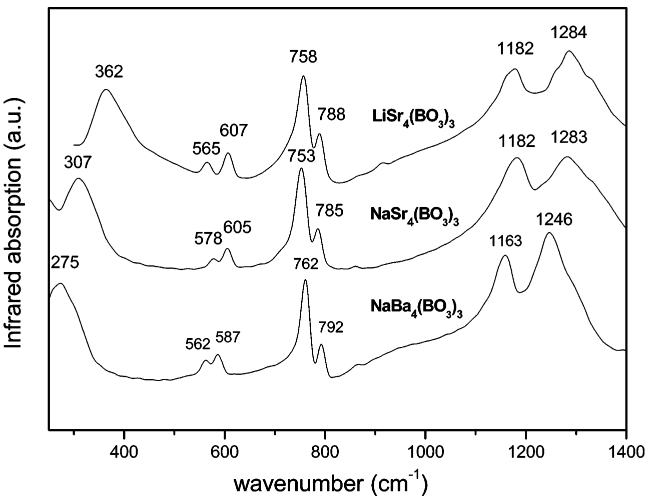

Figure 5. Infrared spectra of LiSr$_4$(BO$_3$)$_3$, NaSr$_4$(BO$_3$)$_3$, and NaBa$_4$(BO$_3$)$_3$.

nm, which is longer than those in the SrB$_4$O$_7$ (367 nm)[7] and BaBe$_2$(BO$_3$)$_2$ (392 nm),[8] comparable to those in the Sr$_3$(BO$_3$)$_2$ (585 nm)[9] and Sr$_2$Mg(BO$_3$)$_2$ (590 nm),[9] and shorter than those in the Ba$_2$Mg(BO$_3$)$_2$ (617 nm)[10] and Ba$_2$LiB$_5$O$_{10}$ (612 nm).[9] The Eu^{2+} luminescence properties in borates can be correlated to the environment of the O atoms in the hosts. Materials with O atoms richly coordinated by Ba or Sr atoms have longer Eu^{2+} emission wavelengths.[11] The yellow emission is in good agreement with the structural studies of MM′$_4$(BO$_3$)$_3$, in which O(1) was coordinated by four Sr or Ba atoms. In addition, the intensity of this yellow luminescence is very dependent on the concentration of europium dopant. With the increasing Eu^{2+} concentration, the intensity of the yellow emission increases and reaches a maximum at about 4 at. %. Above this concentration, the intensity of the yellow emission decreases. It was believed to be the shorter

(19) Rulmont, A.; Almou, M. *Spectrochim. Acta* **1989**, *45A* (5), 603−610.

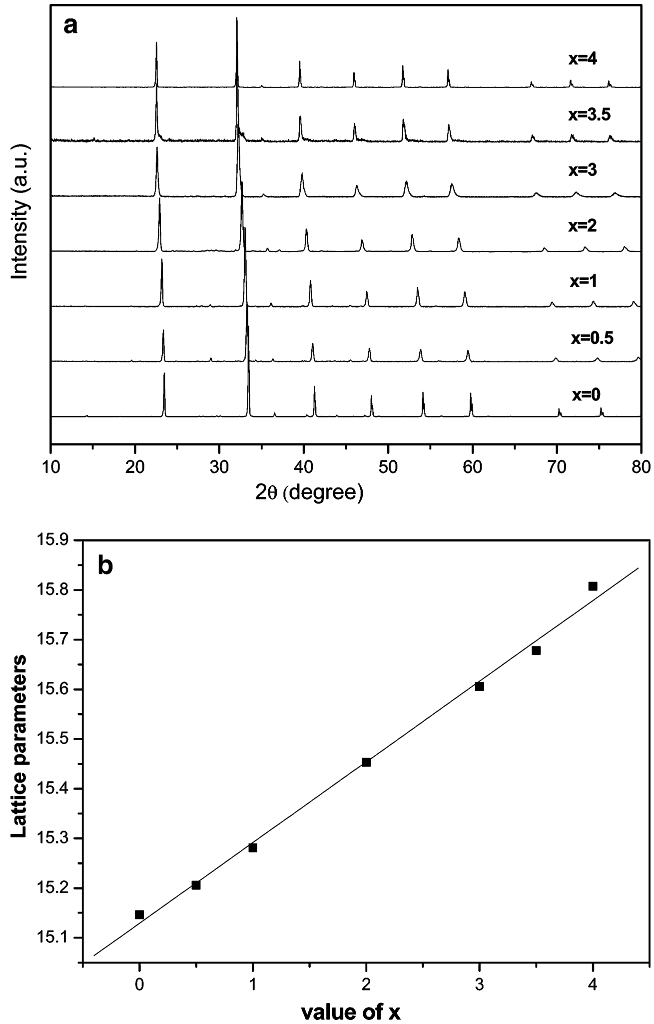

Figure 6. (a) Powder X-ray diffraction patterns of the solid solution NaSr$_{4-x}$Ba$_x$(BO$_3$)$_3$ ($0 \le x \le 4$) with different x values. (b) Variation of lattice parameters on the value of x in NaSr$_{4-x}$Ba$_x$(BO$_3$)$_3$ ($0 \le x \le 4$).

and shorter distance between two Eu^{2+} ions with increasing concentration that induced the concentration quenching.

Samples of MM′$_4$(BO$_3$)$_3$:xEu^{3+} exhibit efficient deep-red emission as shown in Figure 7b. The emission lines ranging from 580 to 720 nm originate from the optical transitions from $^5D_0$ to ^7F_J ($J = 0-4$). The $^5D_0 \rightarrow {}^7F_2$ transition is highly sensitive to structural change and environmental effects and can be used to detect the change in the crystal field. The luminescent spectrum of compact Eu$_2$O$_3$ powder is presented in Figure 7b, which is obviously different from those of MM′$_4$(BO$_3$)$_3$:xEu^{3+}, and proves that the compounds have been successfully doped with Eu^{3+}. Furthermore, the dominant electric dipole−dipole transition at 614 nm ($^5D_0 \rightarrow {}^7F_2$) implies that the Eu^{3+} ion is located in a noncentrosymmetric site in LiSr$_4$(BO$_3$)$_3$:xEu^{3+} and NaSr$_4$(BO$_3$)$_3$:xEu^{3+}. In NaBa$_4$(BO$_3$)$_3$:xEu^{3+}, the magnetic dipole−dipole $^5D_0 \rightarrow {}^7F_1$ transition is predominant; thus, Eu^{3+} should be located in a centrosymmetric position. The Sr/Ba atoms have two sites in the unit cell; one is centrosymmetric (16a) and the other is noncentrosymmetric (48f). We therefore believe that the Eu^{3+} ion prefers to replace the Sr^{2+} in the 48f position in LiSr$_4$(BO$_3$)$_3$ and NaSr$_4$(BO$_3$)$_3$ and the Ba^{2+} in the 16a position in NaBa$_4$(BO$_3$)$_3$. All these observations are in good

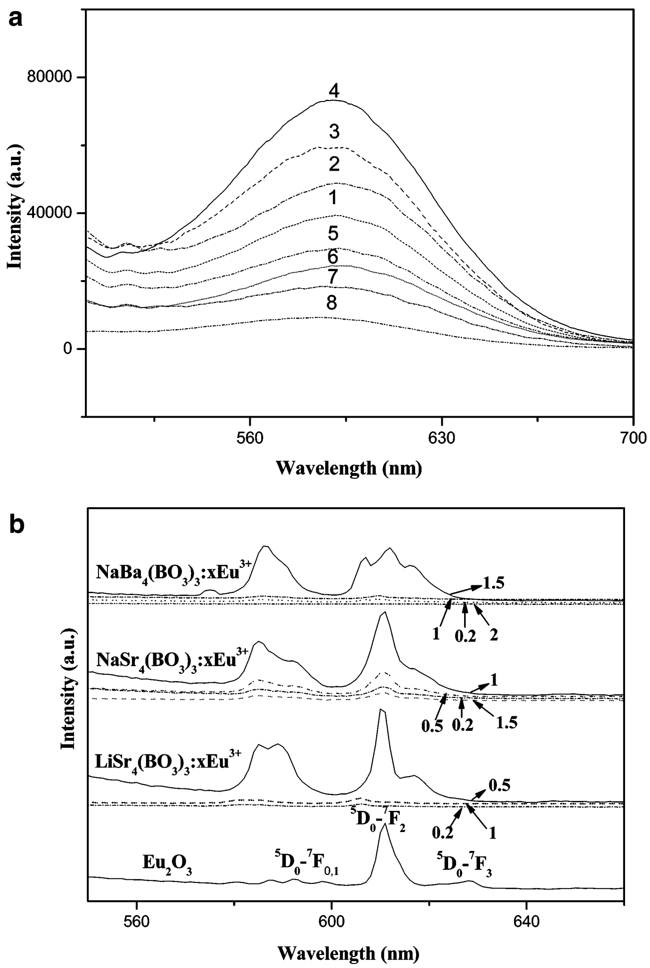

Figure 7. (a) Eu^{2+} concentration dependencies of the luminescence of $LiSr_4(BO_3)_3$:Eu^{2+} ($\lambda_{exc} = 400$ nm) (numbers indicate Eu^{2+} at. %). (b) Eu^{3+} concentration dependencies of the luminescence of compact Eu_2O_3 powder, $LiSr_4(BO_3)_3$:xEu^{3+}, $NaSr_4(BO_3)_3$:xEu^{3+}, and $NaBa_4(BO_3)_3$:xEu^{3+} ($\lambda_{exc} =$ 400 nm) (numbers indicate Eu^{3+} at. %).

agreement with the structural studies. In addition, the luminescent intensity increases with the doping concentration up to $x = 0.5$ at. % for $LiSr_4(BO_3)_3$, $x = 1.0$ at. % for $NaSr_4(BO_3)_3$, and $x = 1.5$ at. % for $NaBa_4(BO_3)_3$, beyond which the luminescence declines very quickly. It is obvious that the quenching concentrations of those Eu^{3+}-doped samples are lower than that of Eu^{2+}-doped samples, especially for the $LiSr_4(BO_3)_3$ (4% for Eu^{2+} and only 0.5% for Eu^{3+}). The reason for so low quenching concentration may be related to the structural distortion induced by substitution of the different valent cation Eu^{3+} for Sr^{2+}/Ba^{2+} in the structure.

Conclusions

Three novel cubic borates, $LiSr_4(BO_3)_3$, $NaSr_4(BO_3)_3$, and $NaBa_4(BO_3)_3$, were synthesized by solid-state reaction, and their structures were solved from powder X-ray diffraction data. In the unit cell, M′ atoms are all located at special positions, separating the unit cell into 64 little cubic grids. Three interperpendicular BO_3 groups and MO_6 cubic octahedra alternately filled in the interspaces of the cubic grids. The M′ atoms appear in two crystallographically different environments, forming distorted octahedral and two-capped trigonal prisms, respectively, sharing edges or planes with each other. Sr and Ba atoms were found to be able to completely substitute each other in the solid solution $NaSr_{4-x}Ba_x(BO_3)_3$ ($0 \le x \le 4$). A series of Eu^{2+}- and Eu^{3+}-doped samples were investigated for luminescence properties, and the results were in good agreement with the crystallographic study. $LiSr_4(BO_3)_3$:Eu^{2+} and $MM'_4(BO_3)_3$:Eu^{3+} show promising yellow and deep-red emission, respectively. But using these borates as the hosts of luminescent materials will need further modification and optimization of the preparation process.

Acknowledgment. This work was financially supported by the National Natural Science Foundation of China (NSFC) under the Grant Nos. 59925206 and 50372081. We thank Mrs. G. R. Liu of the University of Science and Technology Beijing for her great help in collecting powder diffraction data and Mrs. T. Zhou for technical help.

Supporting Information Available: DTA and TGA curves and CIF files for $LiSr_4(BO_3)_3$, $NaSr_4(BO_3)_3$, and $NaBa_4(BO_3)_3$. This material is available free of charge via the Internet at http://pubs.acs.org.

IC050299S